Identification of active erosion areas and areas at risk by remote sensing: an example in the Ésera—Isábena watershed, Central Spanish Pyrenees

L.C. Alatorre [(1)], S. Beguería [(2)], S.M. Vicente Serrano [(1)]

(1) Instituto Pirenaico de Ecología, CSIC, Campus de Aula Dei, Apdo 202, 50080 Zaragoza, España. e-mail: lalatorre@ipe.csic.es
(2) Estación Experimental de Aula Dei, CSIC, Av. Montañana, 1005, 50059, Zaragoza, España.

ABSTRACT
The identification of eroded areas at basin scale can be very useful for environmental planning and can help to reduce land degradation and sediment yield. In this paper remote sensing techniques are used to discriminate eroded areas and areas at risk in a badlands landscape developed on Eocene marls, in the Ésera—Isábena watershed (Spanish Pyrenees). The spatial distribution, the scarce vegetal cover and the high level of erosion let a good visual and digital discrimination of badlands, as opposed to other land covers and surfaces. A maximum likelihood supervised method was used to discriminate heavily eroded areas (badlands) from scarce or densely vegetated lands. The classification distance was used to obtain thresholds for eroded areas and areas at risk. Two error statistics (sensitivity and specificity) where used to determine the most adequate threshold values. The resulting map shows that most areas at risk are located surrounding the badland areas.

Key words: badlands, marls, regolith, statistical sensitivity and specificity.

INTRODUCTION

The term badlands is used to describe areas of unconsolidated sediment or poorly consolidated bedrock, with little or no vegetation. They are typically associated with accelerated erosion and consequent unstable landscapes, so that their fixation requires considerable effort. Badlands develop in a wide range of climatic zones, but particularly in semiarid areas. In sub-humid and humid regions the development of badlands is linked to lithological and topographical factors (Oostwoud-Wijdenes et al., 2000), and to climatic conditions such as freeze–thaw cycles in winter, and wetting–drying in spring–summer. In the Spanish Pyrenees, a combination of favorable relief and climatic conditions is coupled with highly erodible marls outcrops, explaining the presence of badland systems with intense soil erosion processes (Nadal-Romero et al., 2007). The objective of this study was to test a method for identification of areas of severe erosion (badlands) and areas of erosion risk by means of remote sensing classification techniques. The method involved several steps: i) application of a supervised classification algorithm to areas with active erosion features to obtain a map of the spectral distance; ii) selection of a classification threshold based on the ROC curve and error statistics; and iii) assessment of the uncertainty associated with the predictions. The study area corresponded to the corridor of Eocene marls in the middle section of the Ésera—Isábena watershed, in the central Spanish Pyrenees.

STUDY AREA

The study area is located approximately 23 km north of the Barasona reservoir, in the Spanish Pyrenees, and is an integrated badlands landscape developed on Eocene marls orientated north−southeast (Fig. 1) at 620 m to 2149 m altitude. The badlands system is conformed by a group of typical hillside badlands developed on sandy marls with clay soil, and is strongly eroded over convex hillsides with a moderately inclined slope. Runoff from this area enters the Viu and Rialvo rivers in the catchment of the Ésera River, and the Villacarli River in the catchment of the Isábena River.

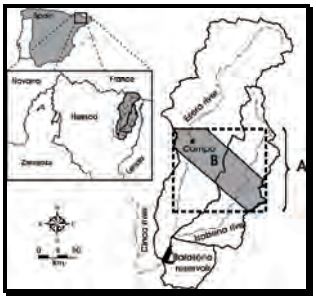

Figure 1. Location of the study area: A, area of the Landsat scene; B, location of badland areas on marls (236 km^2).

Figure 2. Land cover map based on supervised classification using the maximum likelihood method and the maximum probability classification rule.

The climate is defined as mountainous, humid, and cold, with influences from the Atlantic Ocean and the Mediterranean Sea (García-Ruiz et al., 2001). The soils in the study area are chromic Vertisols with an A–B–C profile, an ochric surface horizon, and a C horizon which is typically more than one meter deep. The original parent material is rich in calcium carbonate, accumulated in the form of nodules in the B and C horizons. A significant feature is the formation of cracks arising from shrinkage in the dry season, and these enable mixing of the upper horizon. Under natural conditions, the soils are well protected by a dense vegetation cover, although they suffer occasionally from piping and gullying processes. Disturbance of the vegetation cover leads to accelerated erosion rates and the exposure of the underlying grey marls. These are highly erodible materials, and lead to the formation of a badland morphology (Nadal-Romero et al., 2007).

DATA AND METHODS

In this study Landsat data (spatial resolution 30 m) from August 1st 2006 were used. The image was geometrically corrected using control points and the algorithm developed by Pala and Pons (1996), which accounts for topographic distortion by incorporation of a digital terrain model (DTM). The atmospheric effect on the electromagnetic signal was corrected using the radiative transfer code 6S (Vermote et al., 1997) and the anisotropic reflectance model was used as this is more robust than Lambert's reflectance model (Riaño et al., 2003). Image classification was based on the method of supervised maximum likelihood from the set of 5 thematic classes (Fig. 2). The contingency matrix obtained for the training sample, using the maximum likelihood classification algorithm, showed that all classes had a 90% success value. This allowed to obtain a spectral distance map for the badlands class. Determination of the classification threshold for the construction of maps of active erosion and erosion risk areas was based on the ROC curve, a method coming from the signal processing theory and adapted to environmental applications afterwards (e.g. Beguería, 2006). The ROC curve is constructed by calculating, for each possible classification threshold, the sensitivity and specificity of the resulting classification:

$$sensitivity = \frac{a}{a+c} \quad (1) \qquad specificity = \frac{d}{b+d} \quad (2)$$

where *a* and *d*, respectively, are the true positives and true negatives, and *b* and *c* the false positives and false negatives, respectively. For identification of the active erosion areas (badlands) a classification threshold was set as the spectral distance for which the sensitivity of the model was 0.9, corresponding to a 10% probability of an omission error. For identification of erosion risk areas a classification threshold was set as the spectral distance for which the omission and commission errors were approximately equal (about 25%).

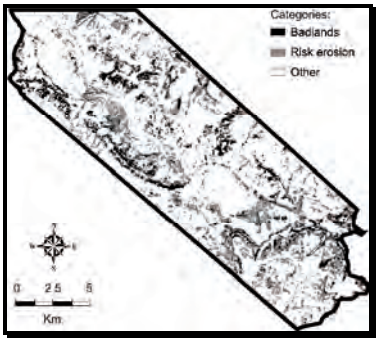

Figure 3. Active erosion (badlands) and erosion risk maps, obtained from the spectral distance map and the classification threshold.

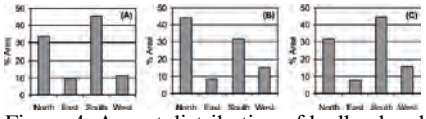

Figure 4. Aspect distribution of badland and erosion risk areas: A, total area; B, badlands area; C, erosion risk area.

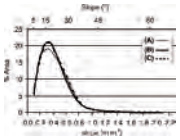

Figure 5.Frequency histogram of hillside slope: A, total area; B, badland areas; C, risk erosion areas.

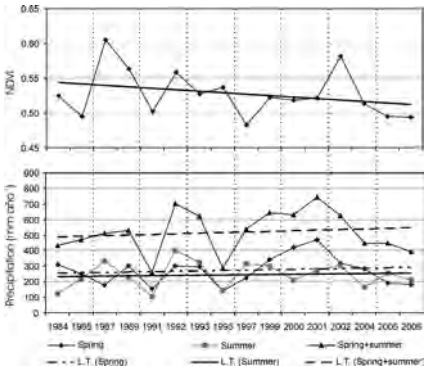

Figure 6. Annual average evolution of the NDVI in the month of August, annual average

RESULTS

The application of both classification thresholds to the map of spectral distance for the badlands class allowed producing maps for the active erosion and risk erosion areas (Fig. 3), with surface areas of these classes of 17 km^2 and 49 km^2, respectively. The surface area of active erosion for the badlands class was the same as that from the land cover map generated previously. Visual comparison of the maps showed that the erosion risk areas corresponded to the scrubland class (and in some cases the grassland and conifer classes) bordering the badlands areas. These areas had spectral characteristics intermediate between badlands and scrubland, indicating either a mixture of the classes within the pixel or an intermediate level of degradation. Both possibilities are consistent with classification of the above classes as erosion risk areas. The DTM morphological analysis showed a predominance of north (33%) and south (45%) orientations over the study area (Fig. 4 A). The badland areas occurred predominantly on hillsides oriented to the north (44%), whereas the erosion risk areas had a distribution similar to the total study area (Fig. 4, C and B). The markedly different distribution of badlands relative to other classes in the study area suggests that different erosion processes are active in opposing hillside orientations. The aspect angle is a determining factor in the dynamics, intensity, and effectiveness of weathering processes in badland areas developing in mountainous sub-humid regions (Nadal-Romero et al., 2007). This is a consequence of regolith weathering dynamics arising from climatic factors (particularly freeze–thaw processes involving cryoclastism, cryosuction, and ice growth) on northorientated hillsides, whereas on south-orientated hillsides the most effective weathering process is thermoclastism, which is related to high daily temperature

variations (Nadal-Romero et al., 2007). Confirmation of this effect would suggest that areas at risk with a north orientation should be a focus for erosion risk mitigation efforts. The frequency distribution of the slope in each class was also analyzed (Fig. 5), but there were no significant differences among the badlands, erosion risk areas, and the total study area. Analysis NDVI (August, 1984-2006) in the zones of risk shows a clear negative tendency (diminution of the vegetal biomass) (Fig. 6), which is not correlated ($p > 0,05$) with the annual average evolution of precipitations (spring, summer, spring + summer) (Fig. 6).

CONCLUSIONS

This study has demonstrated the utility of remote sensing data in basic and applied geomorphologic research, both at watershed and regional scales (study areas between 10 and 10,000 km^2). The use of a supervised classification method based on the maximum likelihood algorithm plus the ROC curve analysis for choosing the most appropriate classification threshold enabled reliable mapping of areas with active erosion. The erosion risk areas bordering the badlands coincided with transition zones from badlands to forest, where the soil was poorly covered by vegetation (10−50% cover). These are marginal areas with slopes greater than 15%, where the establishment of vegetation is very difficult. The DTM was found to be a useful primary tool for morphological exploration of active erosion areas and erosion risk areas. Finally, the annual average evolution of the NDVI (August) in the zones of risk is not correlated with annual average precipitations of the previous months ($p > 0,05$), which suggests these areas are affected by anthropogenic effect. In order to confirm this hypothesis, however, it would be necessary to reject the possible influence of the temperature in the value of the NDVI of August.

ACKNOWLEDGMENTS

This research was financially supported by the projects “Processes and sediment balances at different spatial scales in Mediterranean environments: Effects of climate fluctuations and land use changes” (CGL2006-11619/HID) and “Soil erosion and the Carbon dynamics in Mediterranean agro-ecosystems: radioisotopic modeling at several spatial and temporal scales” (CGL2008-00831/BTE), funded by CICYT, Spanish Ministry of Education and Science. The contribution of the first author has been possible thanks to a scholarship granted by The National Council for Science and Technology of México (CONACYT).

REFERENCES

- Alatorre, L.C. & Beguería, S., 2009. Identification of eroded areas using remote sensing in a badlands landscape on marls in the central Spanish Pyrenees. *Catena* 76, 182–190.
- Beguería S. (2006). Identifying erosion areas at basin scale using remote sensing data and GIS. *International Journal of Remote Sensing*, 20, 4585–4598.
- García-Ruiz, J.M., Beguería, S., López Moreno, J.I., Lorente, A. & Seeger, M. 2001. *Los recursos hídricos superficiales del Pirineo aragonés y su evolución reciente*. Geoforma, Logroño, 192 pp.
- Nadal-Romero, E., Regüés, D., Martí-Bono, C. & Serrano-Muela, P. (2007). Badlands dynamics in the Central Pyrenees: tem-poral and spatial patterns of weathering processes. *Earth Surfaces Processes and Landforms*, 32 (6), 888–904.
- Oostwoud-Wijdenes, D.J., Poesen, J., Vandekerckhove L. & Ghesquiere, M. (2000). Spatial distribution of gully head activity and sediment supply along an ephemeral channel in a Mediterranean environment, *Catena, 39*, 147–167.
- Pala, V. & Pons, X. (1996).Incorporation of relief in polynomial-based geometric corrections. *Photogrammetric enginee-ring & Remote Sensing*, 61(7): 935–944.
- Riaño, D., Chuvieco, E., Salas, J. & Aguado, I. (2003).Assessment of diffe -rent topographic corrections in Landsat TM data for mapping vegetation types. *Geoscience and Remote Sensing, IEEE Transactions*, 41 (5), 1056–1061.
- Vermote, E.F., Tanré, D., Deuzé, J.L., Herman, M. & Morcrette, J.J. (1997). Second simulation of the satellite signal in the solar spectrum, 6s: an overview. *IEEE Transactions on Geoscience and Remote Sensing*, 35 (3), 675–686.